

Article

Algae-Bacteria Community Analysis for Drinking Water Taste and Odour Risk Management

Annalise Sara Hooper^{1,2,*}, Sarah R. Christofides², Fredric M. Windsor², Sophie E. Watson^{1,2}, Peter Kille² and Rupert G. Perkins^{1,2}

¹ School of Earth and Environmental Sciences, Cardiff University, Park Place, Cardiff CF10 3AT, UK; watsons2@cardiff.ac.uk (S.E.W.); perkinsr@cardiff.ac.uk (R.G.P.)

² School of Biosciences, Cardiff University, Sir Martin Evans Building, Museum Avenue, Cardiff CF10 3AX, UK; christofidess@cardiff.ac.uk (S.R.C.); windsorf@cardiff.ac.uk (F.M.W.); kille@cardiff.ac.uk (P.K.)

* Correspondence: hooperas@cardiff.ac.uk; Tel.: +44-7395267130

Abstract: Geosmin and 2-methylisoborneol (2-MIB) are secondary bacterial metabolites that create an earthy-musty taste and odour (T&O) in drinking water. Both compounds exhibit low odour thresholds and are the leading causes of customer complaints to water companies worldwide. Water companies must predict spikes in T&O concentrations early to intervene before these compounds reach the treatment works. Cyanobacteria are key producers of T&O in open waters, yet the influence of broader microbial and algal communities on cyanobacterial T&O events remains unclear. This study identified T&O risk indicator taxa using next-generation sequencing of bacterial (16S rRNA) and algal (*rbcl*) communities in three reservoirs in Wales, UK. Ordination analysis of these communities revealed clustering according to assigned T&O concentration levels, identifying T&O signature communities. Random Forest (RF) analyses accurately classified samples for high and low concentrations of geosmin and 2-MIB, demonstrating the biological consortium's predictive power. Based on shared ecological traits of bacterial and algal taxa, we propose five categories corresponding to different magnitudes of T&O risk. Indicator taxa in T&O risk categories can then be used to predict T&O events, empowering water companies first to optimise treatment response and, importantly, to determine triggers before an event to evidence preventative intervention management.

Keywords: geosmin; 2-MIB; community analysis; taste and odour (T&O); reservoir management



Academic Editors: Yuxue Guo, Jingkai Xie and Hao Chen

Received: 8 December 2024

Revised: 21 December 2024

Accepted: 25 December 2024

Published: 31 December 2024

Citation: Hooper, A.S.; Christofides, S.R.; Windsor, F.M.; Watson, S.E.; Kille, P.; Perkins, R.G. Algae-Bacteria Community Analysis for Drinking Water Taste and Odour Risk Management. *Water* **2025**, *17*, 79. <https://doi.org/10.3390/w17010079>

Copyright: © 2024 by the authors. Licensee MDPI, Basel, Switzerland. This article is an open access article distributed under the terms and conditions of the Creative Commons Attribution (CC BY) license (<https://creativecommons.org/licenses/by/4.0/>).

1. Introduction

The predominant source of customer complaints to drinking water companies worldwide is the earthy-musty flavours imparted by trans-1,10-dimethyl-trans-9-decalol (geosmin) and 2-methylisoborneol (2-MIB) [1–3]. These taste and odour (T&O) compounds exhibit low odour thresholds, with geosmin and 2-MIB ‘events’ defined as water concentrations of $\geq 10 \text{ ng L}^{-1}$ and $\geq 5 \text{ ng L}^{-1}$, respectively [4]. Due to these low concentration thresholds and the high cost of treatment processes such as activated carbon and ozonation [5], water companies aim to limit the production of these compounds in drinking water reservoirs.

Cyanobacterial blooms (i.e., large increases in biomass) have been considered the leading cause of T&O production [6–9]. However, biomass alone does not explain all potential variations in T&O compound concentrations: significant relationships exist between periods of high cyanobacterial productivity and T&O metabolite production, irrespective

of total biomass [10]. Elevated cyanobacterial productivity could explain how some studies have been unsuccessful in correlating T&O compounds with cyanobacterial biomass [11,12]. For example, Kim, et al. [13] found that concentrations of geosmin per unit biomass were maximal when biomass was lowest, but productivity was high. While we know certain environmental conditions influence T&O metabolite production (i.e., high ammonia and low nitrate [4,14], it remains unclear how biological factors at the community level affect cyanobacterial productivity-driven T&O events.

Cyanobacterial productivity is influenced by a variety of factors. A substantial amount of research has focussed on abiotic drivers (e.g., nutrients, temperature, light [15–17]). However, recent work has shown that the wider bacterial communities associated with Cyanobacteria are very influential [18,19]. Heterotrophic bacteria can change the physiochemical properties of the water environments [20], creating favourable/unfavourable environmental conditions for cyanobacterial productivity-driven T&O production. Previous studies revealed that cyanobacterial bloom-associated microbial communities are highly varied at the phylum level [19,21]. However, gene function could be highly conserved despite differences in taxonomic assemblages. It may, therefore, be possible to define cyanobacterial T&O risk categories based on indicator taxa assigned ecological traits such as nitrogen fixation and assimilation [19], organic matter degradation [22], and iron uptake [23]. Former research has focussed on the indirect and direct effects of bacterial communities on cyanobacterial T&O metabolite production [11,22,24]. In doing so, a range of interactions have been observed, all revealing links between certain bacterial communities and increases in the cyanobacterial production of T&O metabolites, including geosmin and 2-MIB. Bacterial communities can also degrade the high molecular weight organic compounds formed by Cyanobacteria [25], constituting key roles in nutrient recycling. Bacterial communities associated with Cyanobacteria can also lower oxygen tension near cyanobacterial cells where oxygen-sensitive biochemical processes (photosynthesis, N-fixation) occur [26]. These interactions may enhance cyanobacterial productivity and, in turn, the production of T&O compounds. Additionally, these bacterial communities participate in other processes that have the potential to promote or inhibit T&O metabolite production by supporting cyanobacterial growth or altering environmental conditions favourable to T&O metabolite release [18,27,28].

Relationships also exist between Cyanobacteria and algae, some of which have the potential to affect productivity. Cyanobacteria provide fixed nitrogen (N) to diatoms in return for amino acids and organic carbon [29–31]. They also help release phosphorus (P) by triggering green algae (Chlorophyta) to secrete alkaline phosphatase (APase), which converts organic P into usable phosphate [32]. Additionally, algal communities help detoxify extracellular iron (Fe) compounds produced by Cyanobacteria, which could otherwise be toxic to the Cyanobacteria in low-oxygen waters [33]. Shared functional traits of algal communities associated with Cyanobacteria could thus accelerate nutrient cycling, facilitate cyanobacterial productivity, and potentially cause a T&O event risk. Although there has been considerable research on communities associated with Cyanobacteria, no studies so far have explored interactions within the broader planktonic communities, including bacteria and algae, or their role in T&O events. This is a crucial gap in our knowledge, as these interactions may affect cyanobacterial T&O metabolite production.

Identifying relationships within communities associated with Cyanobacteria is critical for understanding the mechanisms underlying T&O metabolite production and, ultimately, moving towards predicting T&O events. Advances in molecular methods, particularly correlation-based network analyses, have been successful in exploring microbial community co-occurrence and co-exclusion patterns [34–36]. These molecular techniques, which use the relative abundances of marker genes (e.g., 16S rRNA and *rbcl*), allow the identification of

organisms (and thus potential inter-specific interactions) that were previously impossible to detect, particularly within cyanobacterial and algal communities. Such molecular methods provide novel insights into the complex dynamics of these communities and their roles in T&O events [37]. The co-occurrence of organisms reflects potential positive interactions (e.g., facilitation and mutualisms) and negative interactions (e.g., co-exclusion due to competition for resources or differing environmental preferences) or indicates taxa that share similar environmental niches [38]. The knowledge of both community dynamics and potential interactions afforded by these methods can offer a potential to explore and understand the relationships between communities associated with Cyanobacteria. Investigating such relationships can highlight taxa potentially implicated in T&O production and possibly pinpoint indicative taxa related to increases in geosmin and 2-MIB concentrations.

In this study, next-generation sequencing of 16S rRNA and *rbcL* genes was employed to assess bacterial and algal community dynamics across three drinking water reservoirs in Wales, UK, to explore ecological relationships and identify biotic drivers of T&O events. One reservoir exhibited elevated geosmin concentrations, another showed elevated 2-MIB levels, and the third had neither geosmin nor 2-MIB concentrations exceeding the event threshold, as defined by Hooper, Kille, Watson, Christofides and Perkins [4] (geosmin > 10 ng L⁻¹ and 2-MIB > 5 ng L⁻¹). The research aimed to (1) identify bacterial and algal communities associated with elevated T&O metabolite concentrations; (2) determine whether there are taxa indicative of low and high T&O concentrations; and (3) investigate the co-occurrence networks surrounding T&O-producing Cyanobacteria and understand relationships with environmental factors. The aim was to identify taxa associated with T&O event risk, offering valuable insights for water companies and environmental managers.

2. Materials and Methods

2.1. Reservoir Locations and Sample Collection

Between July 2019 and August 2020, 500 mL of reservoir water (maximum depth 0.5 m) was collected monthly using bankside sampling for molecular analysis from multiple sites in three different reservoirs across Wales, UK (Figure 1). Additional samples were taken simultaneously from the same locations using the same sampling method and used for chemical analysis. Utilising multiple sites in each reservoir reflects a holistic understanding of ecosystem dynamics, capturing the spatial heterogeneity of the reservoirs. This approach allowed for a comprehensive assessment of T&O risk by collating community compositions across the reservoirs. Moreover, it aligns with water quality management practices, which typically examine the reservoir as a single system. The exception to this sampling regime was a sampling break between March and April 2020 due to COVID-19 restrictions. Samples were transported by a refrigerated vehicle and kept at 4 °C before laboratory analysis. During the sampling period, Reservoir 1 (area covered = 360 ha) experienced geosmin events (≤ 520 ng L⁻¹, $n = 32$, sites = 5), Reservoir 2 (area covered = 102 ha, $n = 30$, sites = 2) experienced 2-MIB events (≤ 60 ng L⁻¹) and Reservoir 3 (area covered = 176 ha, $n = 25$, sites = 4) did not experience elevations in either T&O compound (≤ 1.80 ng L⁻¹ for both geosmin and 2-MIB). A summary of geosmin and 2-MIB concentrations for each studied reservoir is provided in Online Resource 1.

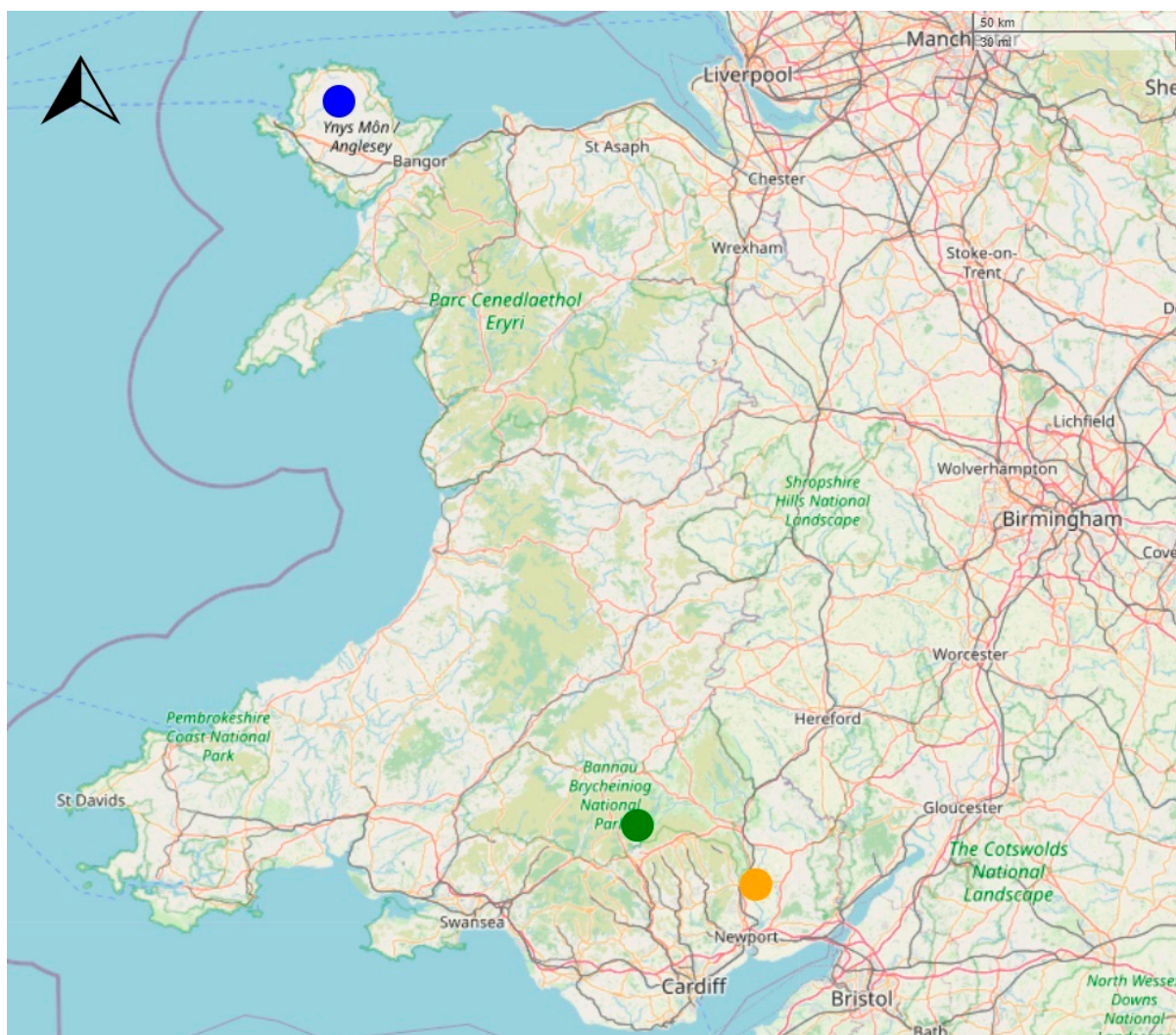


Figure 1. An overview of the studied reservoir locations in Wales (UK). Reservoir locations are coloured as follows: blue for Res-1 (53.3485° N, 4.4233° W; geosmin, five sample points), green for Res-2 (51.8160° N, 3.3706° W; 2-MIB, two sample points) and orange for Res-3 (51.6913° N, 2.9764° W; no T&O events, four sample points). Map created using R 4.4.0 with package ‘leaflet’ [39].

2.2. Geosmin and 2-MIB Concentrations

Gas Chromatography-Tandem Mass Spectrometry (GC-MS/MS) (Agilent, Santa Clara, CA, USA) was used to determine concentrations of geosmin and 2-MIB. Water samples were extracted using a solid phase extraction (SPE) technique at a Dŵr Cymru Welsh Water accredited laboratory (ISO/IEC 17025:2017). Full details of the methodology are listed below [4].

Categorising Geosmin and 2-MIB Concentrations

Low, medium, and high geosmin and 2-MIB concentration categories were proposed to aid data analysis and support the prediction of T&O risk. Drawing distinctions for T&O risk has previously been challenging without clearly defined categories, which are essential for effective modelling and forecasting. By establishing these categories, we can better interpret complex data sets and identify trends or patterns that may indicate forthcoming T&O events. Categories were assigned based on the event-level thresholds set out by Hooper, Kille, Watson, Christofides and Perkins [4] (geosmin $> 10 \text{ ng L}^{-1}$ and 2-MIB $> 5 \text{ ng L}^{-1}$) and are presented in Table 1.

Table 1. T&O concentration category levels for the T&O metabolites, geosmin and 2-MIB.

T&O Compound	Category	Concentrations (ng L ⁻¹)
Geosmin	Low	<5.00
	Medium	5.00–20.00
	High	>20.00
2-MIB	Low	<2.50
	Medium	2.50–10.00
	High	>10.00

2.3. Water Chemistry

Water chemistry measurements were conducted at Dŵr Cymru Welsh Water accredited laboratory in line with ISO/IEC 17025:2017. Ammonium (NH₄⁺), nitrate (NO₃⁻), nitrite (NO₂⁻) and total phosphorus (TP) were analysed using an Aquakem 600 discrete analyser (Thermo Scientific, Waltham, MA, USA) with methods described in [4]. pH was measured via a pH meter using the Skalar SP2000 robot (Skalar Analytical B. V., Breda, The Netherlands). For manganese (Mn) and dissolved iron (DFe), water samples were digested in 1% hydrochloric acid at 85 ± 5 °C overnight before being introduced to the Agilent 7700 Inductively Coupled Plasma Mass Spectrometer (ICP-MS) with a Cetac ASX-500 Autosampler (Agilent Technologies, Santa Clara, CA, USA).

2.4. eDNA Extraction and Next-Generation Sequencing (NGS)

2.4.1. Extracting eDNA from Reservoir Water

Water samples (500 mL) were filtered through a Sterivex filter (0.2 µM) using a vacuum manifold. Then, 1 mL of ATL buffer (Qiagen, Hilden, Germany) was added to the Sterivex filter before storing each sample at -20 °C for later use. Before extraction, 100 µL of proteinase K was added to each filter and left on a turntable for 2 h. DNA was extracted using ~100 µL of the sample removed from each Sterivex filter, following methods described by Fawley and Fawley [40]. Briefly, samples (~100 µL) were mixed with 200 µL of extraction buffer (5M NaCl, 30 mM NaEDTA and 70 mM tris pH 7.0), 25 µL of 10% DTAB and 200 µL of chloroform and added to a tube containing 0.1 mm glass beads. Samples were then agitated using an MP Biomedical, FastPrep-24™ at 5 ms⁻¹ for 30 s twice (with a 5-min incubation at room temperature) before being centrifuged (Eppendorf, Hamburg, Germany, 5417C) at 14,000 rpm for 2 min. The top phase of samples was transferred to a sterile collection tube (200 µL), and 200 µL of buffer AL (Qiagen, Germany) was added along with 200 µL of ethanol before being vortexed for 30 s. DNA was then purified using the procedure and reagents provided within the DNeasy® Blood & Tissue Kit (Qiagen, Germany).

2.4.2. Next Generation Sequencing (NGS): 16S rRNA and *rbcL* Genes

Two gene markers were selected to target algae (*rbcL*) and bacteria (16s rRNA). Initial 16S rRNA and *rbcL* PCRs were carried out on the extracted eDNA samples using primers listed in Table 2 with incorporated Nextera tags on the 5' end of the primers. Compositions of 20 µL PCR reactions were consistent for both target genes, containing 5 µL of 4x AllTaq Mastermix (Qiagen, Hilden, Germany), 0.30 pmol µL⁻¹ of each primer mentioned above and 1 µL of template DNA. PCR reactions were carried out on a SimpliAmp™ Thermal Cycler (Thermo Fisher Scientific, Waltham, MA, USA), using the following conditions: initial denaturation at 95 °C for 2 min followed by 40 cycles of 95 °C for 5 s (denaturation), 55 °C for 15 s (annealing), and 72 °C for 10 s (extension) with a single final extension at 72 °C for 5 min. All reactions were performed in triplicate to account for PCR bias. PCR success was determined using a QIAxcel (Qiagen, Hilden, Germany). The successful

triplicates were subsequently pooled together and underwent a cleaning stage using a Zymo Research 96 DNA clean-up kit (Zymo Research, Cambridge, UK) according to the manufacturer's instructions.

Table 2. Nextera tags and primer sets aused for primary 16S rRNA (bacteria) and *rbcL* (algae) NGS amplifications.

Name	Sequence (5'–3')	Length (Bases)	Amplicon Size (Bases)	Reference
Forward Overhang	TCGTCGGCAGCGTCAGATGTGTATAAGAGACAG	33	-	-
Reverse Overhang	GTCTCGTGGGCTCGGAGATGTGTATAAGAGACAG	34	-	-
<i>rbcL</i> 646F	ATGCGTTGGAGAGARCGTTTC	21	419	[41]
<i>rbcL</i> 998R	GATCACCTTCTAATTTACWACAACCTG	27		
515F	GTGCCAGCMGCCGCGGTAA	19	358	[42]
806R	GGACTACHVGGGTWTCTAAT	20		

Cleaned amplicon samples underwent a secondary amplification to anneal Illumina-Nextera indexes (Illumina, San Diego, CA, USA). 12.5 µL KAPA HiFi HotStart ReadyMix, 5 µL of nuclease-free water and 2.5 µL of each unique Nextera index combination along with 2.5 µL of cleaned primary product. This underwent PCR amplification on a MultiGene™ OptiMax Thermal Cycler (Labnet International, Edison, NJ, USA) using the following conditions: initial denaturation at 95 °C for 3 min followed by eight cycles of 95 °C for 30 s (denaturation), 55 °C for 30 s (annealing), and 72 °C for 30 s (extension) with a single final extension at 72 °C for 5 min.

SequelPrep normalisation plates (Invitrogen, Waltham, USA) were used to normalise the concentrations of the 16S rRNA and *rbcL* amplicons as per the manufacturer's instructions. Before sequencing, normalised samples were pooled together. Samples were sequenced for both genes (16S rRNA and *rbcL*) on separate runs with either an Illumina MiSeq-nano or v2 cartridge using 2 × 250 bp paired-end reads.

2.4.3. Bioinformatic Analysis and Databases for Taxonomic Assignment

Sequence data were processed using QIIME2 v2021.2 [43]. Fastq files from replicate samples were concatenated, and paired-end sequences were demultiplexed and imported into QIIME2. Sequences were denoised, merged, and chimera-checked using the DADA2 pipeline [44]. Run-specific truncation was applied based on read quality scores, and samples from separate runs were merged via amplicon sequence variant (ASV) tables.

Taxonomic assignments were made using two databases: (1) 16S rRNA V4 region (515–806 bp) extracted from the SILVA v132 database [45]; and (2) a custom *rbcL* database, compiled by merging sequences from Diat.barcode v9.2 (accessed 25 October 2021) [46] and GenBank (with overlapping entries removed). GenBank sequences were cross-referenced with NCBI taxdump files for taxonomic classification. Both databases were formatted for QIIME2 and processed using the extract-reads function with a 0.8 identity threshold to filter for primer-containing sequences.

ASV assignment was performed using a Naive Bayes classifier in QIIME2. Post-assignment features were filtered according to the default QIIME parameters to retain those with a minimum relative abundance of 0.1% in at least 0.1% of samples.

2.5. Statistical Analyses

2.5.1. Datasets: Proportional and Binomial Manipulation

All statistical analyses were completed in R 4.1.0 [47]. Sequence data for 16S rRNA and *rbcL* were exported at a genus level (or the closest available lineage/taxonomic rank for unclassified organisms) and converted into proportions separately by calculating the percentage of total reads for each genus based on the total number of reads per sample.

Joint analyses of algae and bacterial communities required the 16S rRNA and *rbcL* proportional datasets to be merged. To do so, we transformed datasets into binomial data to prevent biases towards either group resulting from differences in read depth or amplification efficiencies between bacterial and algal sequences. This transformation allows for a balanced representation of both groups in the analysis, mitigating artefacts that might skew community interactions. Merging different data types in ecological studies is a common approach to reveal broader community dynamics and similar methods have been applied in metabarcoding studies to combine datasets while addressing such biases [48]. Presence (1) was recorded as a taxon proportion $\geq 1\%$ to reduce noise from rare taxa and to focus on ecologically relevant taxa and absence (0) $< 1\%$.

Environmental variables (pH, NH_4^+ , NO_3^- , TP: total phosphorus, DMn: dissolved manganese and DFe: dissolved iron) were converted into categories based on the quartiles of the distribution range of each variable (Q1 ≤ 0.25 , Q2 0.25–0.50, Q3 0.50–0.75 and Q4 > 0.75). Samples with values for each variable that fell into a specific quartile range were marked present (1) and absent (0) for the remaining quartile ranges. This binomial categorisation facilitated analyses alongside the binomial community dataset, enabling comparisons and interpretations of community dynamics in relation to environmental conditions.

2.5.2. Non-Metric Multidimensional Scaling of 16S rRNA and *rbcL* Communities

Non-metric Multi-Dimensional Scaling (NMDS) was used to assess changes in the community structure of 16S rRNA and *rbcL* communities (using proportional data) for reservoirs experiencing geosmin (Reservoir 1) and 2-MIB (Reservoir 2) events. NMDS was calculated using the 'vegan' package [49] using a Bray-Curtis distance, with Wisconsin double standardisation to account for the effects of common and rare taxa. Results were plotted using 'ggplot2' [50].

2.5.3. Random Forest (RF) Models

Random Forest (RF) models were used to identify taxa that could predict low and high T&O risk by classifying samples into low, medium, and high geosmin (for Reservoir 1) and 2-MIB (for Reservoir 2) concentration categories. The purpose of this analysis was to determine which bacterial and algal taxa were most indicative of elevated T&O levels. Using the R package 'randomForest' [51], taxa were treated as independent variables, with the T&O concentration categories as the dependent variable.

The number of trees was first optimised for both reservoirs by running preliminary RFs with 10^5 trees; the point at which the error rate plateaued was selected for subsequent models (10^4 trees for Reservoir 1 and 2×10^3 trees for Reservoir 2). The number of variables used in each tree was optimised by cross-validation using 100 folds. After refining the number of trees and variables (Reservoir 1, $n = 197$ and Reservoir 2, $n = 144$), a final model was run for each reservoir. Multi-dimensional scaling plots were created from the proximity matrices for the geosmin and 2-MIB RFs to assess the models' performance.

To identify indicative organisms relating to T&O levels, taxa in the RF models were ranked in descending order of the Mean Decrease Accuracy (MDA) (the decrease in model accuracy from permutations of each taxon) and the top 20 taxa extracted. The top 20 taxa were used to reduce model complexity, improve model performance and highlight key

indicator taxa. RFs were performed for this subset of taxa for Reservoir 1 (geosmin) and Reservoir 2 (2-MIB), optimising the number of trees (Reservoir 1, 2×10^3 trees and Reservoir 2, 200 trees) and the number of variables used (Reservoir 1, 20 taxa and Reservoir 2, 5 taxa) as described above. Multi-dimensional scaling plots of the proximity matrices from the RFs were again constructed. MDA values associated with the classification of low and high T&O concentrations were further investigated to detect taxa that can differentiate between the two categories (Online Resource 8, geosmin and Online Resource 9, 2-MIB); total mean abundances for each taxon were also calculated to determine average abundances during low and high T&O concentrations.

2.5.4. Co-Occurrence Analyses

To investigate the potential linkages between taxa in the algal and bacterial communities, as well as associations with specific environmental conditions, co-occurrence analyses were performed separately for data from each Reservoir using binomial data and the 'cooccur' package [52] (parameters listed in Online Resource 2). This followed the approach outlined in Faust [38]. Environmental categories (see Section 2.5.1) were included alongside community data to account for the influence of environmental conditions (i.e., a common response to environmental factors) as well as the direct effects of taxa interactions or connectivity [38]. The probabilistic co-occurrence model computes the probability that the co-occurrence between two taxa is either greater or less than expected by chance (i.e., in randomly assembled communities). Specifically, some taxa pairs co-occur more frequently than expected, indicating a higher-than-expected co-occurrence, while others co-occur less frequently, indicating a lower-than-expected co-occurrence. These probabilities should not be treated as P-values in the classical sense, as the co-occurrence networks are an exploratory, hypothesis-generating tool rather than formal inference testing. Instead, a probability threshold of 0.01 was applied to indicate potential interactions of interest. Associations of interest between taxa and environmental categories were extracted and represented as association networks. The nodes in the networks represent taxa and environmental categories, and edges reflect the probability of pairwise associations. Datasets with all nodes and edges used to construct the networks are available in Online Resource 3.

Subnetworks of T&O-producing Cyanobacteria and their associated communities were created to visualise these higher and lower-than-expected co-occurrences. These networks were visualised using 'igraph' [53], 'ggnetwork' [54], and 'ggplot2' [50]. Interactive visualisations of the full networks, created using the 'visNetwork' package [55], are available in Online Resource 4.

2.6. Data Availability

16S rRNA and *rbcl* Next Generation Sequencing data from this study were submitted to the NCBI Sequence Read Archive (SRA) under the accession number PRJNA1080335. All additional data and codes are available on Zenodo (doi:10.5281/zenodo.10671684). More details see the Supplementary Materials.

3. Results

3.1. T&O Categories in NMDS Community Analysis

16S rRNA genera composition in Reservoir 1 (geosmin) revealed distinct communities associated with geosmin levels (Figure 2a). Communities sampled during periods of low and medium geosmin levels did not cluster as distinctively as high geosmin levels and overlapped. Reservoir 2 (2-MIB) 16S rRNA communities also exhibited distinct clustering within the 2-MIB concentration categories (Figure 2b). The community composition for *rbcl* in Reservoir 1 did not appear to cluster according to geosmin levels (Figure 2c). However,

In Reservoir 2 (2-MIB), *rbcL* genera composition can be seen to form a cluster for data points subjected to high 2-MIB levels (Figure 2d).

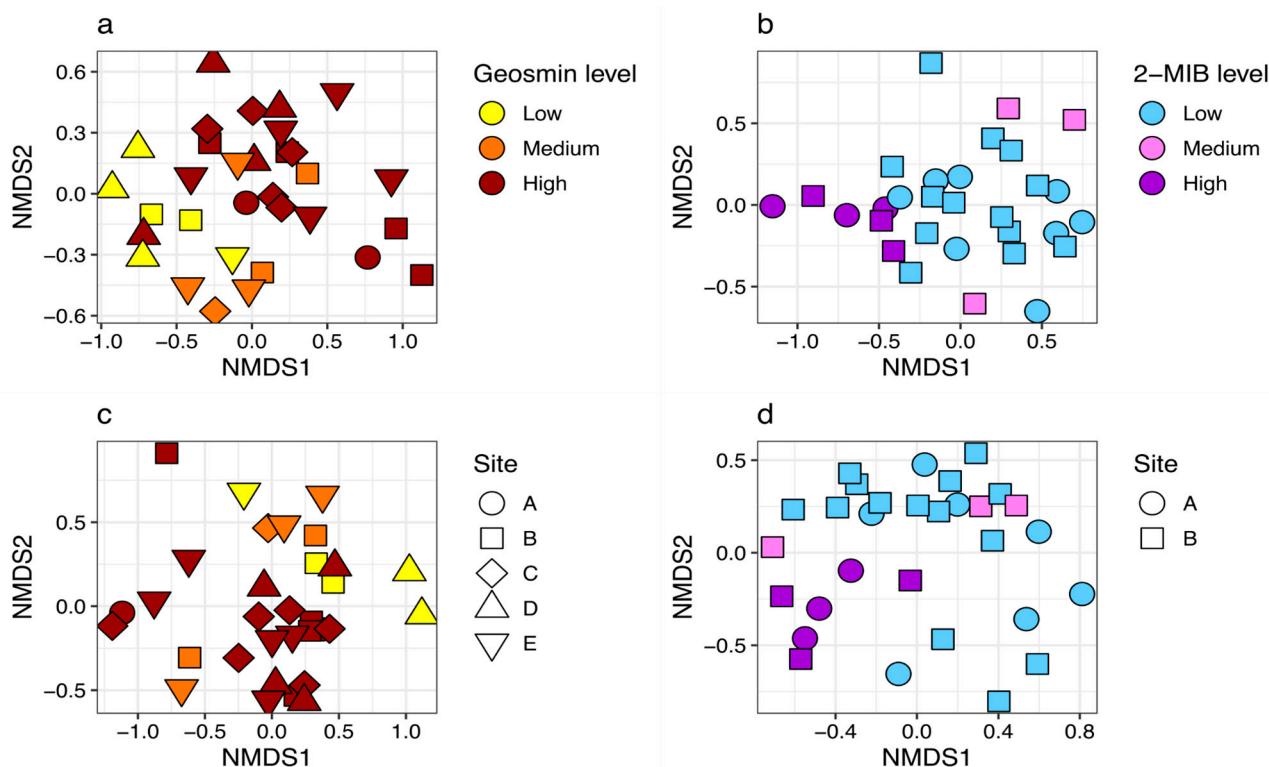


Figure 2. NMDS ordination plots of NGS sequencing data for 16S rRNA for Reservoir 1 (a) $n = 33$ and Reservoir 2 (b) $n = 30$, and for *rbcL* for Reservoir 1 (c) $n = 33$ and Reservoir 2 (d) $n = 30$. Points are coloured according to the T&O category—geosmin in Reservoir 1 and 2-MIB in Reservoir 2—and are shaped by sample point locations.

3.2. Indicative Taxa of T&O ‘Events’ in Reservoirs Experiencing High Geosmin and 2-MIB Concentrations

Random Forest (RF) analysis, using the top 20 taxa as independent variables, correctly classified 100% of samples for high geosmin ($>20.00 \text{ ng L}^{-1}$) and 80% of samples for low geosmin concentrations ($<5 \text{ ng L}^{-1}$) in Reservoir 1. For 2-MIB concentrations in Reservoir 2, RF analysis correctly classified 100% of samples for high ($>10 \text{ ng L}^{-1}$) and low concentrations ($<2.50 \text{ ng L}^{-1}$) (confusion matrices provided in Online Resource 5 and multi-dimensional scaling plots of RF proximity matrices provided in Online Resource 6). For both T&O compounds, the classification of samples for medium concentrations was less accurate (geosmin: $5.00\text{--}20.00 \text{ ng L}^{-1}$ and 2-MIB: $2.50\text{--}10.00 \text{ ng L}^{-1}$). RF classification of samples for medium geosmin concentrations had a 50% error rate for Reservoir 1, and medium concentrations of 2-MIB in Reservoir 2 had a 100% error rate.

T&O Risk Categorisation of Indicative Taxa Identified by RF Analysis

The importance of each taxon from both models was assessed by exploring overall mean decrease accuracy (MDA) values (Online Resource 7). MDA values associated with the classification of low and high T&O concentrations were further investigated to detect taxa that can differentiate between the two categories (Online Resource 8, geosmin and Online Resource 9, 2-MIB); total mean abundances for each taxon were also calculated to determine average abundances during low and high T&O concentrations.

Three Cyanobacteria (*Microcystis* PCC-7914, *Aphanizomenon* NIES81 and *Cyanobium* PCC-6307) were influential in discriminating low and high geosmin concentrations (Reser-

voir 1), although of these, only *Aphanizomenon* NIES81 was itself capable of geosmin production [56]. Interestingly, *Cyanobium* PCC-6307 is a known 2-MIB producer [57], and *Microcystis* PCC-7914 is a known toxin producer of microcystins [11]. *Aphanizomenon* NIES81 was more important in classifying low than high geosmin concentrations; its mean relative abundances show that small proportions of *Aphanizomenon* NIES81 ($0.12 \pm 0.4\%$) are characteristic of low geosmin concentrations, and higher proportions ($14.96 \pm 19.82\%$) are typical of high geosmin concentrations. No relative abundance of *Microcystis* PCC-7914 was recorded during low geosmin concentrations, but this genus received the third-highest MDA value for high geosmin concentrations.

In Reservoir 2, only one 2-MIB-producing Cyanobacteria (*Cyanobium* PCC-6307) was important in classifying low and high 2-MIB concentrations. Three taxa in this model had overall MDA values of 0 (*Legionella*, *Gammaproteobacteria* Class and the *Comamonadaceae* Family) and were disregarded from interpretation.

3.3. Co-Occurrence of Bacterial (16S rRNA) and Algal (*rbcL*) Communities

In Reservoir 1 (geosmin), there were 311 pairwise comparison associations between taxa and environmental variables; 87 pairwise associations exhibited lower-than-expected co-occurrence, and 224 pairwise associations exhibited higher-than-expected co-occurrences (Figure 3a). In this network, there were four co-occurring Cyanobacteria taxa of interest, only two of which are known geosmin producers: *Aphanizomenon* NIES81 and *Nostocaceae* [56]. *Aphanizomenon* NIES81 (Figure 3b) showed higher-than-expected associations with *Fluviicola*, the 2-MIB producer *Cyanobium* PCC-6307 [57], and low concentrations of NO_3^- and NO_2^- and high geosmin concentrations (Figure 3c). *Aphanizomenon* NIES81 also had 13 lower-than-expected associations, including *Bacillus*, a known geosmin-degrading bacterium [58]. Additionally, *Aphanizomenon* NIES81 was associated with lower-than-expected co-occurrence in low pH, high $\text{NO}_3^-/\text{NO}_2^-$ and low geosmin concentrations. The geosmin-producing *Nostocaceae* showed one higher-than-expected association with the *Chlamydomonadaceae* Family and no lower-than-expected co-occurrence associations.

In Reservoir 2 (elevated 2-MIB site), there were 179 pairwise comparisons co-occurrences of interest: 73 pairwise associations showed lower-than-expected co-occurrence, and 106 pairwise associations showed higher-than-expected co-occurrence (Figure 3d). The 2-MIB-producing *Dolichospermum* NIES41 [59] had one higher-than-expected association with the diatom *Melosira*. The 2-MIB producer, *Cyanobium* PCC-6307 [57] exhibited lower-than-expected co-occurrence with five taxa: *Rubinisphaeraceae* Family, *R7C24*, *Gomphonema*, *Ulnaria*, and *Gemmataceae* Family, and higher-than-expected co-occurrence with *Asterionella*, *Sporichyaceae* Family, and *Rhizobiales* A0839 (Figure 3e). *Cyanobium* PCC-6307 also showed lower-than-expected associations with low pH and high dissolved manganese (DMn) and one higher-than-expected co-occurrence with low DMn concentrations. Interestingly, high concentrations of 2-MIB were not associated with Cyanobacteria or any taxon capable of T&O production at a higher or lower-than-expected co-occurrence (Figure 3f).

Additional details on taxa and environmental variables showing higher-than-expected or lower-than-expected co-occurrence with T&O-producing Cyanobacteria in Reservoirs 1 (geosmin) and 2 (2-MIB) are provided in Online Resources 10 and 11.

In Reservoir 3 (no concentrations of geosmin or 2-MIB above event level threshold), there were 224 pairwise comparisons co-occurrences of interest; 66 pairwise associations were lower-than-expected, while 158 pairwise associations were higher-than-expected (Figure 3g). In Reservoir 3, only two Cyanobacteria displayed co-occurrences: the 2-MIB-producing *Cyanobium* PCC-6307 and *Aphanizomenon* MDT14a (not a known geosmin producer according to genome analysis by Driscoll [60]) (Figure 3h). Interestingly, the Cyanobacteria present in Reservoir 3's network exhibited more higher-than-expected

pairwise co-occurrences compared to the T&O-producing Cyanobacteria in Reservoirs 1 and 2, which had a higher frequency of lower-than-expected associations. For *Cyanobium* PCC-6307, higher-than-expected co-occurrences existed with *Aphanizomenon* MDT14a, *Sporichthyaceae* Family, *Limnohabitans*, and *Fragilaria*, as well as high pH and low TP and DFe concentrations. This community network had one lower-than-expected co-occurrence with *Schlesneria* and low pH and NO_2^- concentrations. The potential importance of these taxa and environmental variables associated with the 2-MIB-producing *Cyanobium* PCC-6307 is summarised in Online Resource 12.

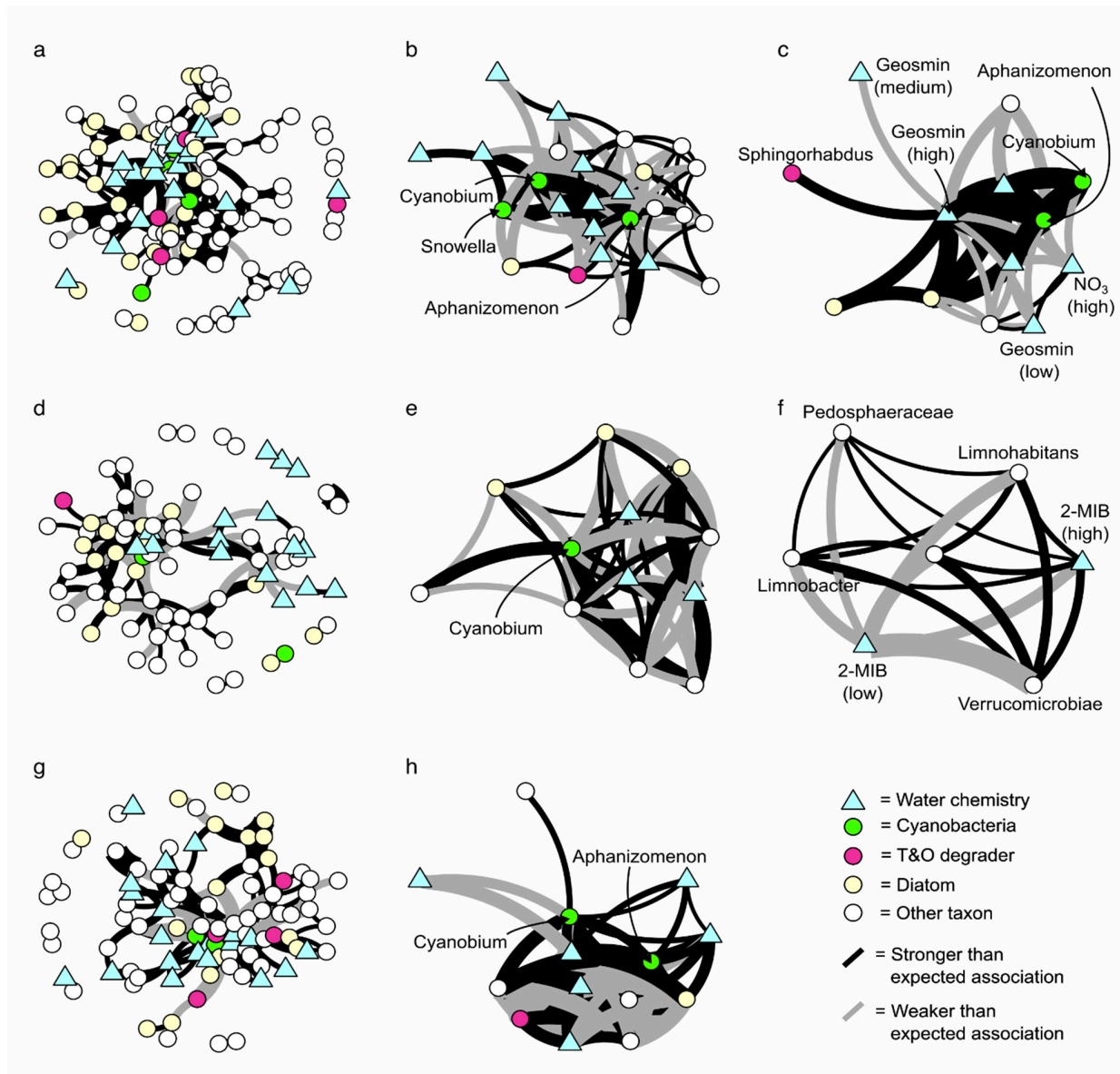


Figure 3. Overview of co-occurring taxa and environmental categories of interest for Reservoirs 1 (a–c), 2 (d–f), and 3 (g), (h) based on combined 16S rRNA and *rbcL* data. Panels B, E, and H display subsets of T&O-producing Cyanobacteria: *Aphanizomenon* NIES81 (B-Reservoir 1-geosmin), *Cyanobium* PCC-6307 (E-Reservoir 2, 2-MIB), and *Cyanobium* PCC-6307 and *Aphanizomenon* MDT14a (H-Reservoir 3, no T&O events). Panels C and F show the networks directly surrounding high levels of both geosmin and 2-MIB for Reservoirs 1 and 2, respectively. Cyanobacterial nodes are green, T&O-degrading bacterial nodes are purple, diatom nodes are yellow, and environmental categories are represented by blue triangles. Edges indicate lower-than-expected co-occurrences (grey lines) and higher-than-expected co-occurrences (black lines), with line thickness reflecting the strength of the association.

3.4. T&O Risk Indicator Categories and Associated Taxa

The literature searches of taxa identified by RF models for Reservoir 1 (geosmin) and Reservoir 2 (2-MIB) (Section 3.2) were conducted, and ecological functions were examined. T&O risk categories were then established based on the shared ecological functions of key taxa identified in the RF models (Table 3). These categories were further applied to taxa co-occurring with T&O-producing Cyanobacteria, organising taxa into the same categories (Table 3).

Table 3. T&O Risk Categories for Taxa Influencing Potential Cyanobacterial Geosmin and 2-MIB Production Based on Shared Ecological Traits.

T&O Risk Category	Key Taxa Identified by RF Analysis		Key Taxa Co-Occurring with T&O-Producing Cyanobacteria	
	Geosmin	2-MIB	Geosmin	2-MIB
Cyanobacterial T&O Producers	<i>Aphanizomenon</i> NIES81	<i>Cyanobium</i> PCC-6307	<i>Aphanizomenon</i> NIES81, Nostocaceae	<i>Cyanobium</i> PCC-6307, <i>Dolichospermum</i> NIES41
T&O Degraders	<i>Pseudomonas</i> , <i>Bacillus</i>	<i>Limnobacter</i>	<i>Bacillus</i>	-
Nutrient Enrichment Indicators ⁸⁷	Peptostreptococcaceae , <i>Vicinamibacterales</i> Order, <i>Melosira</i>	<i>Armatimonas</i> , <i>Nitzschia</i>	Peptostreptococcaceae , <i>Aulacoseira</i>	<i>Asterionella</i> , <i>Melosira</i>
Nutrient Exchange/Recycling	-	<i>Limnohabitans</i> , NS9 <i>marine group</i> , Gemmataceae	<i>Fluviicola</i> , Chlamydomonadaceae	Gemmataceae , <i>Rhizobiales</i> A0939
Cyanobacterial Benefactors	OM27 Clade	<i>Sediminibacterium</i> , OM190	-	-

Note: Bold names represent taxa that both co-occur with T&O-producing Cyanobacteria and identified in RF analysis.

4. Discussion

This study is the first to explore T&O risk associated with Cyanobacteria by integrating bacterial and algal communities in combination with environmental datasets to identify indicator taxa organised into T&O-risk categories. Identifying bacterial and algal signature communities of low, medium, and high T&O concentration categories indicates that T&O risk can be inferred from these communities. In addition, RF analysis revealed that T&O-producing Cyanobacteria are influential in distinguishing between low and high T&O concentrations and critical threshold extremes for water companies in managing water quality. Community network analysis was consistent with findings from the RF analysis, identifying T&O-producing Cyanobacteria from Reservoir 1 (geosmin) and Reservoir 2 (2-MIB) to be associated with high T&O concentration categories, thereby identifying the potential source of T&O metabolite production. T&O-producing Cyanobacteria in Reservoir 1 (geosmin) and Reservoir 2 (2-MIB) experienced lower-than-expected co-occurrences with other taxa, suggesting that they are less frequently associated with other taxa in a stable or cooperative manner; this could indicate a more selective or unstable ecological role of these T&O-producing Cyanobacteria in the community. The unstable community structure associated with T&O-producing Cyanobacteria may influence their physiology, with T&O metabolite production potentially linked to stress-induced conditions. However, T&O production as a stress response can only occur during the right environmental conditions (low NO_3^- and NO_2^-). In contrast, co-occurring T&O-producing Cyanobacteria of interest with

other taxa present in Reservoir 3 (no T&O events) exhibited a greater frequency of higher-than-expected co-occurrences with other taxa. T&O-producing Cyanobacteria in Reservoir 3 may display a more stable or integrated role, indicating stronger or more predictable associations with other taxa within Reservoir 3's ecosystem. In identifying taxa from RF and community network analysis, we propose T&O-risk categories based on the shared function-specific traits of the indicator taxa (T&O-risk categories are discussed below).

4.1. Categorisation of Indicative Taxa for T&O Risk

Ordination analysis revealed that bacterial (16S rRNA) and algal (*rbcL*) communities clustered by T&O concentration categories (low, medium and high) across Reservoir 1 (geosmin) and Reservoir 2 (2-MIB), indicating that the biology consortium as a response to water quality can reflect T&O concentrations. Both bacteria and algae display T&O signature communities, where specific taxa are associated with T&O concentration categories. From combining data from these communities, indicative taxa associated with T&O-risk were identified in a reservoir experiencing extreme geosmin concentrations (Reservoir 1 ≤ 520 ng L⁻¹) and in a reservoir with moderate 2-MIB concentrations (Reservoir 2 ≤ 60 ng L⁻¹). Indicative taxa for the differentiation between low and high T&O metabolite concentrations were identified, and T&O risk categories were constructed based on the shared ecological functions of each taxon. These categories were further applied to include the taxa associated with T&O-producing Cyanobacteria from community network analysis. Here, five T&O risk categories are proposed and are summarised below; the taxa associated with each category are detailed in Table 3 for reference.

4.1.1. Cyanobacterial T&O Producers

For a T&O event to occur, Cyanobacteria that possess the genes encoding geosmin synthase (*geoA*) and/or 2-MIB cyclase (*mic*) must be present within the community under appropriate environmental conditions, such as low NO₃⁻ and NO₂⁻ concentrations as observed in this study. *Aphanizomenon* NIES81 was an important variable in the RF model analysis for categorising geosmin concentrations. RF results from Reservoir 2 indicated that *Cyanobium* PCC-6307 was associated with the presence of 2-MIB, suggesting that this Cyanobacteria could be responsible for 2-MIB production. In this study, both *Aphanizomenon* NIES81 (Reservoir 1) and *Cyanobium* PCC-6307 (Reservoir 2) exhibited more lower-than-expected co-occurrences with other community members than higher-than-expected co-occurrences. These lower-than-expected associations imply biotic stress (induced by unstable ecological associations) may trigger the production of T&O metabolites, with geosmin and 2-MIB potentially serving as a defence mechanism, as sesquiterpenoids have previously been implicated in cellular defence [61]. In Reservoir 1, *Aphanizomenon* NIES81 was associated with low NO₃⁻, NO₂⁻, and high geosmin concentrations, consistent with previous findings indicating maximal geosmin production when oxidised nitrogen forms are scarce [15]. Thus, the presence of T&O-producing Cyanobacteria is likely influenced by biotic stress and/or specific nutrient conditions, such as a low NO₃⁻:NH₄⁺ ratio, which may stimulate both cyanobacterial growth and T&O metabolite production [4].

4.1.2. T&O Degraders

Elevations in T&O metabolite compounds are hypothesised to select different bacterial species capable of degrading these compounds, thereby increasing the likelihood of such degradation processes occurring. Clercin, et al. [62] observed elevations in geosmin concentrations in a eutrophic reservoir were associated with *Novosphingobium hassiacum* and *Sphingomonas oligophenolica*, whereas increased concentrations of 2-MIB were linked to *Flavobacterium* species. The roles of *Pseudomonas* and *Bacillus* in T&O compound degradation remained unclear [62], despite evidence of their capacity to degrade both com-

pounds [63–65]. In this study, the geosmin-degrading *Pseudomonas* had a greater influence on the RF classification of high rather than low geosmin concentrations in Reservoir 1 (geosmin). The mean relative abundance of *Pseudomonas* increased during times of high geosmin concentrations compared to low, implying that increases in this degrader could indicate a T&O risk. Three strains of the T&O degrader, *Pseudomonas*, have also been reported to contain the geosmin synthase gene (*geoA*), although it is not known if they are effective geosmin producers [66]. It is unknown why most species of *Pseudomonas* lack the genes to produce geosmin. In contrast, *Bacillus* in Reservoir 1 (geosmin) occurred at a lower-than-expected frequency with *Aphanizomenon* NIES81 and was an important variable in the RF model analysis for categorising geosmin concentrations. T&O degraders like *Bacillus* have been shown to display an antagonistic relationship with a previously described geosmin-producing strain of *Streptomyces* [65], which agrees with previous findings from natural communities [67,68]. The increased abundance of *Bacillus* would thus be characteristic after periods of high T&O. A potential 2-MIB degrader identified in this study that needs further investigation is *Limnobacter*. In Reservoir 2 (2-MIB), RF analysis revealed *Limnobacter* as the most informative genus in categorising 2-MIB concentrations into low and high categories, with heightened relative abundance in *Limnobacter* during high 2-MIB concentrations. It has been postulated that *Limnobacter* species can degrade a vast array of aromatic compounds [69,70], although there are no reports to date of this genus degrading T&O compounds.

T&O degraders have the potential to cause fluctuations in geosmin and 2-MIB concentrations in water columns, depending on the relative rates of cyanobacterial T&O production and the biodegradation of the T&O metabolites.

4.1.3. Nutrient Enrichment Indicators

Nutrient enrichment indicators are taxa that tend to be present during periods of nutrient enrichment. For instance, the *Peptostreptococcaceae* family has been identified as an indicator of nutrient enrichment in urban lakes [71]. In Reservoir 1 (geosmin), *Peptostreptococcaceae* exhibited a lower-than-expected co-occurrence with *Aphanizomenon* NIES81 despite having the greatest influence on the RF model's performance in classifying low versus high geosmin concentrations. The enrichment of nutrients such as NH_4^+ could trigger the cyanobacterial production of T&O metabolite compounds like geosmin [14]. The presence of *Peptostreptococcaceae* before a T&O event suggests a potential early indicator of T&O risk. The lower-than-expected co-occurrence with *Aphanizomenon* NIES81 in Reservoir 1's community network could be explained by niche overlap, as both taxa are capable of nitrogen fixation [72]. This overlap may lead to competitive exclusion, where these organisms compete for similar ecological resources, potentially reducing their co-occurrence within the same habitat. Another indicator of nutrient enrichment is the diatom genus *Melosira*, which is commonly associated with eutrophic and polluted aquatic systems [73]. In the studied reservoirs, *Melosira* played a significant role in the RF analysis for classifying low and high geosmin concentrations. Additionally, *Melosira* exhibited a higher-than-expected co-occurrence with the 2-MIB-producing cyanobacterium *Dolichospermum* NIES41 in Reservoir 2 (2-MIB), suggesting a potential ecological interaction between these taxa under nutrient-enriched conditions. *Armatimonas* was also significant in the RF classification of low and high geosmin concentrations in Reservoir 1, consistent with previous studies linking this taxon to geosmin production after increases in TP concentrations [74]. Elevations in TP concentrations favour cyanobacterial growth and productivity, and consequential shifts in the total nitrogen (TN) to TP ratio—particularly TN ratios below 30:1—have been associated with increased geosmin production in reservoirs [15].

Additionally, the diatom *Nitzschia*, known for its association with nutrient-enriched waters and sensitivity to nutrient depletion [75], was influential in the RF classification of low and high 2-MIB concentrations in Reservoir 2. In Reservoir 2, declines in *Nitzschia* abundance were indicative of heightened 2-MIB risk. Additional diatoms characteristic of nutrient enrichment are *Aulacoseira* and *Asterionella* [75]. *Aulacoseira* displayed lower-than-expected co-occurrence with *Aphanizomenon* NIES81 in Reservoir 1 (geosmin). However, according to Reynolds, Huszar, Kruk, Naselli-Flores and Melo [75], this is to be expected due to their sensitivity to rising pH values associated with increased cyanobacterial productivity [76]. In contrast, *Asterionella* had a higher-than-expected co-occurrence with *Cyanobium* PCC-6307 in Reservoir 2 (2-MIB), rapid increases in *Asterionella* species can deplete major anions (NO_3^- , PO_4^{3-} and silicates), leading to altered nutrient ratios [77].

4.1.4. Nutrient Exchange/Recycling

Taxa capable of nutrient exchange and recycling can benefit Cyanobacteria by creating favourable conditions that promote the production of secondary metabolites, such as geosmin and 2-MIB [78]. For example, in Reservoir 2, *Limnohabitans* had a higher-than-expected co-occurrence with *Cyanobium* PCC-6307 and was highly influential in classifying low and high 2-MIB concentrations. The primary growth substrates for *Limnohabitans* are autochthonous algal/cyanobacterial organic matters and products from the photolysis of dissolved materials [79]; culture-independent analyses show this genus to constitute 11% of the cyanobacterial phycosphere [80]. The NS9 marine group was also an important variable in categorising low and high 2-MIB concentrations in Reservoir 2. The growth of these prokaryotes is associated with phytoplanktonic organic matter [81] and have been identified to degrade polysaccharides [82]. Similarly, previous work has identified *Gemmataceae* to contain wide repertoires of carbohydrate-active enzymes, allowing them to utilise some polysaccharides, such as xylan, laminarin, lichenin and starch [83]. *Gemmataceae* had a lower-than-expected co-occurrence with *Cyanobium* PCC-6307 in Reservoir 2 but was influential in categorising 2-MIB concentrations into low and high categories. Another taxon affiliated with the nutrient exchange/recycling for 2-MIB-producing *Cyanobium* PCC-6307 was *Rhizobiales* A0839. Previous studies link this taxon with NH_4^+ oxidation and removal in wastewater treatment [84]. This is an unusual pairing as both taxa compete for NH_4^+ , although previous evidence suggests that NH_4^+ -oxidising bacteria deny Cyanobacteria access to NH_4^+ and force diazotrophic Cyanobacteria into nitrogen fixation mode [85]. However, forced cyanobacterial nitrogen fixation in *Cyanobium* PCC-6307 cannot be assumed to be fuelling 2-MIB production in Reservoir 2 without further investigation, as the majority of 2-MIB-producing Cyanobacteria are thought to be non-heterocyst producing [86].

The only higher-than-expected co-occurring taxon with *Aphanizomenon* NIES81 in Reservoir 1 was *Fluviicola*. *Fluviicola* is affiliated with the family *Cryomorpaceae*, which belongs to the class *Flavobacteriia* and contains many species that play an integral role in the recycling of carbon and energy in freshwater environments [87]. *Flavobacteriia* are major decomposers of high-molecular-mass organic matter in water bodies [88], like the 2-MIB degrading genus *Flavobacterium* [62]. Guedes, et al. [89] have previously shown *Fluviicola* to have positive correlations with *Synechococcus*, following previous findings from natural communities [67,68]. The *Chlamydomonadaceae* family co-occurred at a higher-than-expected probability with the *Nostocaceae* family in Reservoir 1; this family contains the genus *Chlamydomonas*. Although no reports suggest that the *Nostocaceae* family can produce cylindrospermopsin, Kust, et al. [90] stated that *Nostocaceae* are a rich source of unknown secondary metabolites that require further investigation. These metabolites could have a similar effect to cylindrospermopsin on members of the *Chlamydomonadaceae* family, inducing the algae to produce APases for the Cyanobacteria to use.

4.1.5. Cyanobacterial Benefactors

Sediminibacterium has been shown to offer Cyanobacteria protection against the colonisation of opportunistic bacteria by producing bacteriocin and toxoflavin [91]. *Sediminibacterium* can also form biofilm consortia with Cyanobacteria [92], and its relationship with Cyanobacteria in wastewater has also been previously reported [93]. In this study, *Sediminibacterium* was considered more influential on the RF model's performance in classifying high than low 2-MIB concentrations. Another taxon influential in categorising 2-MIB concentrations was the genus *OM190*. This taxon produces a diverse range of secondary metabolites, including antimicrobial compounds [94], which have the potential to protect Cyanobacteria from undesired microbes. Protection of T&O-producing Cyanobacteria would, in turn, enhance T&O risk. For the categorisation of low and high geosmin concentrations, the *OM27* clade was highly influential in the model's performance, especially for high geosmin concentrations. Members of the *OM27* clade are known to prey on opportunistic bacteria [95] and have been shown to dominate the bacterioplankton community during cyanobacterial blooms [96]. We hypothesise that members of the *OM27* clade predate on opportunistic bacteria alongside Cyanobacteria, enabling them to become more resilient in the community, which in turn can present a T&O risk.

5. Conclusions

This study marks the first to investigate T&O risk linked to Cyanobacteria by integrating bacterial and algal data to identify indicator taxa for T&O-risk categories. The analysis of bacterial and algal communities in reservoirs with elevated geosmin and 2-MIB concentrations revealed distinct T&O signature communities. The identification of bacterial and algal communities associated with low, medium, and high T&O concentration categories suggests that T&O risk can be inferred from these communities. By combining bacterial and algal datasets, key taxa distinguishing between low and high T&O concentration categories were identified.

T&O-producing Cyanobacteria in Reservoir 1 (geosmin) and Reservoir 2 (2-MIB) showed fewer dependable associations with other taxa, indicating a selective or unstable ecological role. This instability may trigger T&O metabolite production as a stress response under specific environmental conditions, such as low NO_3^- and NO_2^- levels. Conversely, Cyanobacteria in the reservoir without T&O events exhibited more stable interactions with other taxa, suggesting a more integrated ecological role.

These findings underscore the importance of cyanobacterial interactions within the broader microbial community and the potential of using indicator taxa to assess T&O risk. This approach provides valuable insights for water companies and environmental managers, enabling more accurate predictions and management of T&O events. Importantly, enhanced predictive capability also better identifies triggers of T&O metabolite production prior to events occurring after a temporal lag (between metabolite production and T&O event at the Water treatment works) and is hence of key importance in drinking water resource management.

Supplementary Materials: The following supporting information can be downloaded at: <https://www.mdpi.com/article/10.3390/w17010079/s1>. References [15,32,57,58,60,65,71,73,75,77,83,84,89,97–125] are cited in the Supplementary Materials.

Author Contributions: A.S.H.: Conceptualization, methodology, validation, formal analysis, investigation, resources, data curation, writing—original draft, writing—review and editing, and visualisation; S.R.C.: Conceptualization, methodology, validation, formal analysis, data curation, writing—review and editing, visualisation; F.M.W.: Methodology, validation, review and editing, visualisation; S.E.W.: Writing—conceptualisation, review and editing; P.K.: Conceptualization, method-

ology, formal analysis, investigation, resources, writing—original draft, writing—review and editing, supervision, project administration, funding acquisition; R.G.P.: Conceptualization, investigation, resources, writing—original draft, writing—review and editing, supervision, project administration, funding acquisition. All authors have read and agreed to the published version of the manuscript.

Funding: This work was supported by funding from the NERC Centre for Doctoral Training in Freshwater Biosciences and Sustainability from the Natural Environment Research Council [NE/R0115241].

Data Availability Statement: 16S rRNA and *rbcL* Next Generation Sequencing data from this study were submitted to the NCBI Sequence Read Archive (SRA) under the accession number PRJNA1080335. All additional data and code are available on Zenodo (doi:10.5281/zenodo.10671684).

Acknowledgments: A.S.H collaborated with Dŵr Cymru, Welsh Water (DCWW). The authors would like to acknowledge the significant assistance of Gemma Godwin and Greg Bullock, together with the rest of the DCWW Catchment Management Team and the analytical team at the DCWW Glaslyn laboratories.

Conflicts of Interest: The authors have no relevant financial or non-financial interests to disclose.

References

1. Devi, A.; Chiu, Y.T.; Hsueh, H.T.; Lin, T.F. Quantitative PCR based detection system for cyanobacterial geosmin/2-methylisoborneol (2-MIB) events in drinking water sources: Current status and challenges. *Water Res.* **2021**, *188*, 116478. [[CrossRef](#)] [[PubMed](#)]
2. Pochiraju, S.; Hoppe-Jones, C.; Adams, C.; Weinrich, L. Development and optimization of analytical methods for the detection of 18 taste and odor compounds in drinking water utilities. *Water Res. X* **2021**, *11*, 100099. [[CrossRef](#)] [[PubMed](#)]
3. Wu, T.; Zhu, G.; Wang, Z.; Zhu, M.; Xu, H. Seasonal dynamics of odor compounds concentration driven by phytoplankton succession in a subtropical drinking water reservoir, southeast China. *J. Hazard. Mater.* **2022**, *425*, 128056. [[CrossRef](#)] [[PubMed](#)]
4. Hooper, A.S.; Kille, P.; Watson, S.E.; Christofides, S.R.; Perkins, R.G. The importance of nutrient ratios in determining elevations in geosmin synthase (*geoA*) and 2-MIB cyclase (*mic*) resulting in taste and odour events. *Water Res.* **2023**, *232*, 119693. [[CrossRef](#)] [[PubMed](#)]
5. Mustapha, S.; Tijani, J.O.; Ndamitso, M.; Abdulkareem, A.S.; Shuaib, D.T.; Mohammed, A.K. A critical review on geosmin and 2-methylisoborneol in water: Sources, effects, detection, and removal techniques. *Environ. Monit. Assess.* **2021**, *193*, 204. [[CrossRef](#)]
6. Adams, H.; Southard, M.; Reeder, S.; Buerkens, F.; Hallford, R.L.; Ikehata, K.; Nix, D.K. Successfully Detecting and Mitigating Algal Blooms and Taste and Odor Compounds. *J. AWWA* **2021**, *113*, 10–19. [[CrossRef](#)]
7. Bruder, S.; Babbar-Sebens, M.; Tedesco, L.; Soyeux, E. Use of fuzzy logic models for prediction of taste and odor compounds in algal bloom-affected inland water bodies. *Environ. Monit. Assess.* **2014**, *186*, 1525–1545. [[CrossRef](#)]
8. Hayes, K.P.; Burch, M.D. Odorous compounds associated with algal blooms in South Australian water. *Water Res.* **1989**, *23*, 115–121. [[CrossRef](#)]
9. Newton, R.J.; Jones, S.E.; Eiler, A.; McMahon, K.D.; Bertilsson, S.; Yamada, Y.; Kuzuyama, T.; Komatsu, M.; Shin-ya, K.; Omura, S.; et al. Chemotactic and Growth Responses of Marine Bacteria to Algal Extracellular Products. *PLoS ONE* **2015**, *10*, 265–277.
10. Zimmerman, W.J.; Soliman, B.H.; Rosen, B.H. Growth and 2-methylisoborneol production by the cyanobacterium *Phormidium* LM689. *Water Sci. Technol.* **1995**, *31*, 181–186. [[CrossRef](#)]
11. Graham, J.L.; Loftin, K.A.; Meyer, M.T.; Ziegler, A.C. Cyanotoxin mixtures and taste-and-odor compounds in cyanobacterial blooms from the midwestern united states. *Environ. Sci. Technol.* **2010**, *44*, 7361–7368. [[CrossRef](#)] [[PubMed](#)]
12. Watson, S.B.; Ridal, J.; Boyer, G.L. Taste and odour and cyanobacterial toxins: Impairment, prediction, and management in the Great Lakes. *Can. J. Fish. Aquat. Sci.* **2008**, *65*, 1779–1796. [[CrossRef](#)]
13. Kim, K.; Park, C.; Yoon, Y.; Hwang, S.J. Harmful cyanobacterial material production in the north han river (South Korea): Genetic potential and temperature-dependent properties. *Int. J. Environ. Res. Public Health* **2018**, *15*, 444. [[CrossRef](#)]
14. Perkins, R.G.; Slavin, E.I.; Andrade, T.M.C.; Blenkinsopp, C.; Pearson, P.; Froggatt, T.; Godwin, G.; Parslow, J.; Hurley, S.; Luckwell, R.; et al. Managing taste and odour metabolite production in drinking water reservoirs: The importance of ammonium as a key nutrient trigger. *J. Environ. Manag.* **2019**, *244*, 276–284. [[CrossRef](#)]
15. Harris, T.D.; Smith, V.H.; Graham, J.L.; Waa, D.B.V.d.; Tedesco, L.P.; Clercin, N. Combined effects of nitrogen to phosphorus and nitrate to ammonia ratios on cyanobacterial metabolite concentrations in eutrophic Midwestern USA reservoirs. *Inland Waters* **2016**, *6*, 199–210. [[CrossRef](#)]

16. Montgomery, B.L. The regulation of light sensing and light-harvesting impacts the use of cyanobacteria as biotechnology platforms. *Front. Bioeng. Biotechnol.* **2014**, *2*, 22. [[CrossRef](#)]
17. Robarts, R.D.; Zohary, T. Temperature effects on photosynthetic capacity, respiration, and growth rates of bloom—Forming cyanobacteria. *New Zealand J. Mar. Freshw. Res.* **1987**, *21*, 391–399. [[CrossRef](#)]
18. Salomon, P.S.; Janson, S.; Granéli, E. Molecular identification of bacteria associated with filaments of *Nodularia spumigena* and their effect on the cyanobacterial growth. *Harmful Algae* **2003**, *2*, 261–272. [[CrossRef](#)]
19. Louati, I.; Pascault, N.; Debroas, D.; Bernard, C.; Humbert, J.F.; Leloup, J. Structural diversity of bacterial communities associated with bloom-forming freshwater cyanobacteria differs according to the cyanobacterial genus. *PLoS ONE* **2015**, *10*, e0140614. [[CrossRef](#)]
20. Havens, K.E. Cyanobacteria blooms: Effects on aquatic ecosystems. *Adv. Exp. Med. Biol.* **2008**, *619*, 733–747.
21. Steffen, M.M.; Li, Z.; Effler, T.C.; Hauser, L.J.; Boyer, G.L.; Wilhelm, S.W. Comparative Metagenomics of Toxic Freshwater Cyanobacteria Bloom Communities on Two Continents. *PLoS ONE* **2012**, *7*, e44002. [[CrossRef](#)] [[PubMed](#)]
22. Berg, K.A.; Lyra, C.; Sivonen, K.; Paulin, L.; Suomalainen, S.; Tuomi, P.; Rapala, J. High diversity of cultivable heterotrophic bacteria in association with cyanobacterial water blooms. *ISME J.* **2009**, *3*, 314–325. [[CrossRef](#)] [[PubMed](#)]
23. Ploug, H.; Adam, B.; Musat, N.; Kalvelage, T.; Lavik, G.; Wolf-Gladrow, D.; Kuypers, M.M.M. Carbon, nitrogen and O₂ fluxes associated with the cyanobacterium *Nodularia spumigena* in the Baltic Sea. *ISME J.* **2011**, *5*, 1549–1558. [[CrossRef](#)] [[PubMed](#)]
24. Youn, S.J.; Kim, H.N.; Yu, S.J.; Byeon, M.S. Cyanobacterial occurrence and geosmin dynamics in Paldang Lake watershed, South Korea. *Water Environ. J.* **2020**, *34*, 634–643. [[CrossRef](#)]
25. Cai, H.; Jiang, H.; Krumholz, L.R.; Yang, Z. Bacterial Community Composition of Size-Fractionated Aggregates within the Phycosphere of Cyanobacterial Blooms in a Eutrophic Freshwater Lake. *PLoS ONE* **2014**, *9*, e102879. [[CrossRef](#)]
26. Paerl, H.W.; Kellar, P.E. Significance of bacterial (cyanophyceae) *Anabaena* associations with respect to N₂ fixation in freshwater. *J. Phycol.* **1978**, *14*, 254–260. [[CrossRef](#)]
27. Simon, M.; Grossart, H.-P.; Schweitzer, B.; Ploug, H. Microbial ecology of organic aggregates in aquatic ecosystems. *Aquat. Microb. Ecol.* **2002**, *28*, 175–211. [[CrossRef](#)]
28. Eiler, A.; Bertilsson, S. Composition of freshwater bacterial communities associated with cyanobacterial blooms in four Swedish lakes. *Environ. Microbiol.* **2004**, *6*, 1228–1243. [[CrossRef](#)]
29. Foster, R.A.; Kuypers, M.M.M.; Vagner, T.; Paerl, R.W.; Musat, N.; Zehr, J.P. Nitrogen fixation and transfer in open ocean diatom-cyanobacterial symbioses. *ISME J.* **2011**, *5*, 1484–1493. [[CrossRef](#)]
30. Hilton, J.A.; Foster, R.A.; James Tripp, H.; Carter, B.J.; Zehr, J.P.; Villareal, T.A. Genomic deletions disrupt nitrogen metabolism pathways of a cyanobacterial diatom symbiont. *Nat. Commun.* **2013**, *4*, 1767. [[CrossRef](#)]
31. Thompson, A.W.; Foster, R.A.; Krupke, A.; Carter, B.J.; Musat, N.; Vaulot, D.; Kuypers, M.M.; Zehr, J.P. Unicellular cyanobacterium symbiotic with a single-celled eukaryotic alga. *Science* **2012**, *6101*, 1546–1560. [[CrossRef](#)] [[PubMed](#)]
32. Bar-Yosef, Y.; Sukenik, A.; Hadas, O.; Viner-Mozzini, Y.; Kaplan, A. Enslavement in the water body by toxic aphanizomenon ovalisporum, inducing alkaline phosphatase in phytoplanktons. *Curr. Biol.* **2010**, *20*, 1557–1561. [[CrossRef](#)] [[PubMed](#)]
33. Paerl, H.W.; Pinckney, J.L. A mini-review of microbial consortia: Their roles in aquatic production and biogeochemical cycling. *Microb. Ecol.* **1996**, *31*, 225–247. [[CrossRef](#)]
34. Barberán, A.; Bates, S.T.; Casamayor, E.O.; Fierer, N. Using network analysis to explore co-occurrence patterns in soil microbial communities. *ISME J.* **2012**, *6*, 343–351. [[CrossRef](#)]
35. Eiler, A.; Heinrich, F.; Bertilsson, S. Coherent dynamics and association networks among lake bacterioplankton taxa. *ISME J.* **2012**, *6*, 330–342. [[CrossRef](#)]
36. Ju, F.; Zhang, T. Bacterial assembly and temporal dynamics in activated sludge of a full-scale municipal wastewater treatment plant. *ISME J.* **2015**, *9*, 683–695. [[CrossRef](#)]
37. Faust, K.; Raes, J. Microbial interactions: From networks to models. *Nat. Rev. Microbiol.* **2012**, *10*, 538–550. [[CrossRef](#)]
38. Faust, K. Open challenges for microbial network construction and analysis. *ISME J.* **2021**, *15*, 3111–3118. [[CrossRef](#)]
39. Cheng, J.; Karambelkar, B.; Xie, Y. leaflet: Create Interactive Web Maps with the JavaScript ‘Leaflet’ Library. 2017. Available online: <https://rstudio.r-universe.dev/leaflet> (accessed on 7 December 2024).
40. Fawley, M.W.; Fawley, K.P. A simple and rapid technique for the isolation of DNA from microalgae. *J. Phycol.* **2004**, *40*, 223–225. [[CrossRef](#)]
41. Glover, R. Biomonitoring and Surveillance with Short-and Long-Read Metabarcoding. Ph.D. Thesis, University of Exeter, Exeter, UK, 2019.
42. Caporaso, J.G.; Lauber, C.L.; Walters, W.A.; Berg-Lyons, D.; Lozupone, C.A.; Turnbaugh, P.J.; Fierer, N.; Knight, R. Global patterns of 16S rRNA diversity at a depth of millions of sequences per sample. *Proc. Natl. Acad. Sci. USA* **2011**, *108*, 4516–4522. [[CrossRef](#)]
43. Bolyen, E.; Rideout, J.R.; Dillon, M.R.; Bokulich, N.A.; Abnet, C.C.; Al-Ghalith, G.A.; Alexander, H.; Alm, E.J.; Arumugam, M.; Asnicar, F.; et al. Reproducible, interactive, scalable and extensible microbiome data science using QIIME 2. *Nat. Biotechnol.* **2019**, *37*, 852–857. [[CrossRef](#)] [[PubMed](#)]

44. Callahan, B.J.; McMurdie, P.J.; Rosen, M.J.; Han, A.W.; Johnson, A.J.A.; Holmes, S.P. DADA2: High-resolution sample inference from Illumina amplicon data. *Nat. Methods* **2016**, *13*, 581–583. [CrossRef] [PubMed]
45. Callahan, B.J. Silva Taxonomic Training Data Formatted for DADA2 (Silva Version 132). [Dataset]. 2018. Available online: <https://zenodo.org/records/1172783> (accessed on 7 December 2024).
46. Rimet, F.; Gusev, E.; Kahlert, M.; Kelly, M.G.; Kulikovskiy, M.; Maltsev, Y.; Mann, D.G.; Pfannkuchen, M.; Trobajo, R.; Vasselon, V.; et al. Diat.barcode, an open-access curated barcode library for diatoms. *Sci. Rep.* **2019**, *9*, 15116. [CrossRef] [PubMed]
47. R_Core_Team. *R: A Language and Environment for Statistical Computing*; R Foundation for Statistical Computing: Vienna, Austria, 2021.
48. Cuff, J.P.; Windsor, F.M.; Tercel, M.P.T.G.; Kitson, J.J.N.; Evans, D.M. Overcoming the pitfalls of merging dietary metabarcoding into ecological networks. *Methods Ecol. Evol.* **2022**, *13*, 545–559. [CrossRef]
49. Oksanen, J. Vegan: Ecological diversity. *R Proj.* **2013**, *368*, 1–11.
50. Wickham, H. *ggplot2. Use R! In Data Analysis*; Springer: Cham, Switzerland, 2016; pp. 1–13.
51. Breiman, L. Random Forests. *Mach. Learn.* **2001**, *45*, 5–32. [CrossRef]
52. Veech, J.A. A probabilistic model for analysing species co-occurrence. *Glob. Ecol. Biogeogr.* **2013**, *22*, 252–260. [CrossRef]
53. Csardi, G.; Nepusz, T. The Igraph Software Package for Complex Network Research. 2006, 1695. Available online: https://www.researchgate.net/publication/221995787_The_Igraph_Software_Package_for_Complex_Network_Research (accessed on 7 December 2024).
54. Briatte, F. ggnetwork: Geometries to Plot Networks with 'ggplot2'. 2023. Available online: <https://briatte.github.io/ggnetwork/> (accessed on 7 December 2024).
55. Almende, B.; Thieurmel, B.; Robert, T. visNetwork: Network Visualization Using 'vis. js' Library. R Package Version 2.0.9. 2019, 1–105. Available online: <https://cran.r-project.org/web/packages/visNetwork/visNetwork.pdf> (accessed on 7 December 2024).
56. Driscoll, C.B.; Meyer, K.A.; Šulčius, S.; Brown, N.M.; Dick, G.J.; Cao, H.; Gasiūnas, G.; Timinskas, A.; Yin, Y.; Landry, Z.C.; et al. A closely-related clade of globally distributed bloom-forming cyanobacteria within the Nostocales. *Harmful Algae* **2018**, *77*, 93–107. [CrossRef]
57. Jakubowska, N.; Szeląg-Wasielewska, E. Toxic picoplanktonic cyanobacteria—Review. *Mar. Drugs* **2015**, *13*, 1497–1518. [CrossRef]
58. Zhi, Y.; Wu, Q.; Du, H.; Xu, Y. Biocontrol of geosmin-producing *Streptomyces* spp. by two *Bacillus* strains from Chinese liquor. *Int. J. Food Microbiol.* **2016**, *231*, 1–9. [CrossRef]
59. Zhang, J.; Li, L.; Qiu, L.; Wang, X.; Meng, X.; You, Y.; Yu, J.; Ma, W. Effects of Climate Change on 2-Methylisoborneol Production in Two Cyanobacterial Species. *Water* **2017**, *9*, 859. [CrossRef]
60. Driscoll, C.B. Comparative Genomics of Freshwater Bloom-Forming Cyanobacteria and Associated Organisms. 2016. Available online: [https://www.pacificorp.com/content/dam/pcorp/documents/en/pacificorp/energy/hydro/klamath-river/khsa-implementation/technical-documents/2016-DNA-Special-Study\(Final_4-12-17\).pdf](https://www.pacificorp.com/content/dam/pcorp/documents/en/pacificorp/energy/hydro/klamath-river/khsa-implementation/technical-documents/2016-DNA-Special-Study(Final_4-12-17).pdf) (accessed on 7 December 2024).
61. Pattanaik, B.; Lindberg, P. Terpenoids and Their Biosynthesis in Cyanobacteria. *Life* **2015**, *5*, 269–293. [CrossRef] [PubMed]
62. Clercin, N.A.; Druschel, G.K.; Gray, M. Occurrences of 2-methylisoborneol and geosmin –degrading bacteria in a eutrophic reservoir and the role of cell-bound versus dissolved fractions. *J. Environ. Manag.* **2021**, *297*, 113304. [CrossRef]
63. Eaton, R.W.; Sandusky, P. Biotransformations of (+/–)-geosmin by terpene-degrading bacteria. *Biodegradation* **2010**, *21*, 71–79. [CrossRef]
64. Ho, L.; Hoefel, D.; Bock, F.; Saint, C.P.; Newcombe, G. Biodegradation rates of 2-methylisoborneol (MIB) and geosmin through sand filters and in bioreactors. *Chemosphere* **2007**, *66*, 2210–2218. [CrossRef]
65. Ma, N.N.; Luo, G.Z.; Tan, H.X.; Yao, M.L.; Wange, X.Y. Kinetic Characteristics of Degradation of Geosmin and 2-Methylisoborneol by *Bacillus subtilis*. *Huan Jing Ke Xue* **2015**, *36*, 1379–1384.
66. Churro, C.; Semedo-Aguiar, A.P.; Silva, A.D.; Pereira-Leal, J.B.; Leite, R.B. A novel cyanobacterial geosmin producer, revising GeoA distribution and dispersion patterns in Bacteria. *Sci. Rep.* **2020**, *10*, 8679. [CrossRef]
67. Bertos-Fortis, M.; Farnelid, H.M.; Lindh, M.V.; Casini, M.; Andersson, A.; Pinhassi, J.; Legrand, C. Unscrambling cyanobacteria community dynamics related to environmental factors. *Front. Microbiol.* **2016**, *7*, 625. [CrossRef]
68. Salmaso, N.; Albanese, D.; Capelli, C.; Boscaini, A.; Pindo, M.; Donati, C. Diversity and Cyclical Seasonal Transitions in the Bacterial Community in a Large and Deep Perialpine Lake. *Microb. Ecol.* **2018**, *76*, 125–143. [CrossRef]
69. Pérez-Pantoja, D.; Donoso, R.; Agulló, L.; Córdova, M.; Seeger, M.; Pieper, D.H.; González, B. Genomic analysis of the potential for aromatic compounds biodegradation in Burkholderiales. *Environ. Microbiol.* **2012**, *14*, 1091–1117. [CrossRef]
70. Vedler, E.; Heinaru, E.; Jutkina, J.; Viggor, S.; Koressaar, T.; Remm, M.; Heinaru, A. Limnobacter spp. as newly detected phenol-degraders among Baltic Sea surface water bacteria characterised by comparative analysis of catabolic genes. *Syst. Appl. Microbiol.* **2013**, *36*, 525–532. [CrossRef] [PubMed]
71. Numberger, D.; Zoccarato, L.; Woodhouse, J.; Ganzert, L.; Sauer, S.; Márquez, J.R.G.; Domisch, S.; Grossart, H.P.; Greenwood, A.D. Urbanization promotes specific bacteria in freshwater microbiomes including potential pathogens. *Sci. Total Environ.* **2022**, *845*, 157321. [CrossRef] [PubMed]

72. Paster, B.J.; Russell, J.B.; Yang, C.M.J.; Chow, J.M. Phylogeny of the Ammonia-Producing Ruminal Bacteria. *Int. J. Syst. Bacteriol.* **1993**, *43*, 107–110. [CrossRef] [PubMed]
73. Van de Vijver, B.; Crawford, R.M. *Melosira jeanbertrandiana*, a new *Melosira* species (Bacillariophyceae) from the sub-Antarctic region. *Bot. Lett.* **2020**, *167*, 50–56. [CrossRef]
74. Xu, Z.; Te, S.H.; He, Y.; Gin, K.Y.H. The characteristics and dynamics of cyanobacteria-heterotrophic bacteria between two estuarine reservoirs—Tropical versus subtropical regions. *Front. Microbiol.* **2018**, *9*, 2531. [CrossRef]
75. Reynolds, C.S.; Huszar, V.; Kruk, C.; Naselli-Flores, L.; Melo, S. Towards a functional classification of the freshwater phytoplankton. *J. Plankton Res.* **2002**, *24*, 417–428. [CrossRef]
76. Slavin, E. Using Artificial Circulation for In-Reservoir Management of Cyanobacteria and Taste and Odour Metabolite Production. 2020, 1–248. Available online: <https://www.fao.org/fishery/en/openasfa/b6727947-d718-4bbe-860f-af0a258e2c33> (accessed on 7 December 2024).
77. Krivtsov, V.; Bellinger, E.G.; Sigee, D.C. Changes in the elemental composition of *Asterionella formosa* during tim diatom spring bloom. *J. Plankton Res.* **2000**, *22*, 169–184. [CrossRef]
78. Wu, L.; Zhang, C.; Vadiveloo, A.; Montes, M.L.; Xia, L.; Song, S.; Fernandez, M.A.; Lan, S. Efficient nutrient recycling from wastewater to deserts: A comparative study on biocrust cyanobacteria performance. *Chem. Eng. J.* **2024**, *491*, 151927. [CrossRef]
79. Ye, Q.; Liu, J.; Du, J.; Zhang, J. Bacterial Diversity in Submarine Groundwater along the Coasts of the Yellow Sea. *Front Microbiol* **2016**, *6*, 1519. [CrossRef]
80. Kim, M.; Lee, J.; Yang, D.; Park, H.Y.; Park, W. Seasonal dynamics of the bacterial communities associated with cyanobacterial blooms in the Han River. *Environ. Pollut.* **2020**, *266*, 115198. [CrossRef]
81. Takebe, H.; Tominaga, K.; Isozaki, T.; Watanabe, T.; Yamamoto, K.; Kamikawa, R.; Yoshida, T. Taxonomic difference in marine bloom-forming phytoplanktonic species affects the dynamics of both bloom-responding prokaryotes and prokaryotic viruses. *mSystems* **2024**, *9*, e00949-23. [CrossRef] [PubMed]
82. Reintjes, G.; Heins, A.; Wang, C.; Amann, R. Abundance and composition of particles and their attached microbiomes along an Atlantic Meridional Transect. *Front. Mar. Sci.* **2023**, *10*, 1051510. [CrossRef]
83. Kulichevskaya, I.S.; Ivanova, A.A.; Naumoff, D.G.; Beletsky, A.V.; Rijpstra, W.I.C.; Sinninghe Damsté, J.S.; Mardanov, A.V.; Ravin, N.V.; Dedysh, S.N. *Frigoriglobus tundricola* gen. nov., sp. nov., a psychrotolerant cellulolytic planctomycete of the family Gemmataceae from a littoral tundra wetland. *Syst. Appl. Microbiol.* **2020**, *43*, 126129. [CrossRef] [PubMed]
84. Rodriguez-Sanchez, A.; Muñoz-Palazon, B.; Hurtado-Martinez, M.; Maza-Marquez, P.; Gonzalez-Lopez, J.; Vahala, R.; Gonzalez-Martinez, A. Microbial ecology dynamics of a partial nitrification bioreactor with Polar Arctic Circle activated sludge operating at low temperature. *Chemosphere* **2019**, *225*, 73–82. [CrossRef]
85. Boyett, M.R.; Tavakkoli, A.; Sobolev, D. Mathematical Modeling of Competition for Ammonium among Bacteria, Archaea and Cyanobacteria within Cyanobacterial Mats: Can Ammonia- Oxidizers Force Nitrogen Fixation ? *Ocean Sci. J.* **2013**, *48*, 269–277. [CrossRef]
86. Jeong, J.Y.; Lee, S.H.; Yun, M.R.; Oh, S.E.; Lee, K.H.; Park, H.D. 2-Methylisoborneol (2-Mib) Excretion By *Pseudanabaena Yagii* Under Low Temperature. *Microorganisms* **2021**, *9*, 486. [CrossRef]
87. Woyke, T.; Chertkov, O.; Lapidus, A.; Nolan, M.; Lucas, S.; del Rio, T.G.; Tice, H.; Cheng, J.F.; Tapia, R.; Han, C.; et al. Complete genome sequence of the gliding freshwater bacterium *Fluviicola taffensis* type strain (RW262T). *Stand. Genom. Sci.* **2011**, *5*, 21–29. [CrossRef]
88. Cottrell, M.T.; Kirchman, D.L. Natural assemblages of marine proteobacteria and members of the Cytophaga-flavobacter cluster consuming low- and high-molecular-weight dissolved organic matter. *Appl. Environ. Microbiol.* **2000**, *66*, 1692–1697. [CrossRef]
89. Guedes, I.A.; Rachid, C.T.C.C.; Rangel, L.M.; Silva, L.H.S.; Bisch, P.M.; Azevedo, S.M.F.O.; Pacheco, A.B.F. Close link between harmful cyanobacterial dominance and associated bacterioplankton in a tropical eutrophic reservoir. *Front. Microbiol.* **2018**, *9*, 424. [CrossRef]
90. Kust, A.; Urajová, P.; Hrouzek, P.; Vu, D.L.; Čapková, K.; Štenclová, L.; Řeháková, K.; Kozlíková-Zapomělová, E.; Lepšová-Skácelová, O.; Lukešová, A.; et al. A new microcystin producing *Nostoc* strain discovered in broad toxicological screening of non-planktic Nostocaceae (cyanobacteria). *Toxicon* **2018**, *150*, 66–73. [CrossRef]
91. Sethuraman, A.; Stancheva, R.; Sanders, C.; Caceres, L.; Castro, D.; Hausknecht-Buss, H.; Henry, S.; Johansen, H.; Kasler, A.; Lastor, S.; et al. Genome of a novel Sediminibacterium discovered in association with two species of freshwater cyanobacteria from streams in Southern California. *G3 Genes Genomes Genet.* **2022**, *12*, jkac123. [CrossRef] [PubMed]
92. Velichko, N.; Chernyaeva, E.; Averina, S.; Gavrilova, O.; Lapidus, A.; Pinevich, A. Consortium of the 'bichlorophyllous' cyanobacterium *Prochlorothrix hollandica* and chemoheterotrophic partner bacteria: Culture and metagenome-based description. *Environ. Microbiol. Rep.* **2015**, *7*, 623–633. [CrossRef] [PubMed]
93. Lee, J.; Lee, J.; Lee, T.K.; Woo, S.G.; Baek, G.S.; Park, J. In-depth characterization of wastewater bacterial community in response to algal growth using pyrosequencing. *J. Microbiol. Biotechnol.* **2013**, *23*, 1472–1477. [CrossRef] [PubMed]

94. Pushpakumara, B.L.D.U.; Tandon, K.; Willis, A.; Verbruggen, H. Unravelling microalgal-bacterial interactions in aquatic ecosystems through 16S co-occurrence networks. *Sci. Rep.* **2022**, *13*, 2743.
95. Orsi, W.D.; Smith, J.M.; Liu, S.; Liu, Z.; Sakamoto, C.M.; Wilken, S.; Poirier, C.; Richards, T.A.; Keeling, P.J.; Worden, A.Z.; et al. Diverse, uncultivated bacteria and archaea underlying the cycling of dissolved protein in the ocean. *ISME J.* **2016**, *10*, 2158–2173. [[CrossRef](#)]
96. Wang, K.; Razzano, M.; Mou, X. Cyanobacterial blooms alter the relative importance of neutral and selective processes in assembling freshwater bacterioplankton community. *Sci. Total Environ.* **2020**, *706*, 135724. [[CrossRef](#)]
97. Newitt, J.T. Roles and Recruitment of Streptomyces Species in the Wheat Root Microbiome. 2020, 1–241. Available online: <https://ueaeprints.uea.ac.uk/id/eprint/81445/1/2020NewittJPhDPhD.pdf> (accessed on 7 December 2024).
98. Rajaneesh, K.M.; Naik, R.K.; Roy, R.; Costa, P.M.D. Cyanobacteria in tropical and subtropical marine environments: Bloom formation and ecological role. In *Advances in Cyanobacterial Biology*; Academic Press: Cambridge, MA, USA, 2020; pp. 35–46.
99. Yuan, Q.; Wang, P.; Wang, X.; Hu, B.; Tao, L. Phytoremediation of cadmium-contaminated sediment using *Hydrilla verticillata* and *Elodea canadensis* harbor two same keystone rhizobacteria Pedosphaeraceae and Parasegetibacter. *Chemosphere* **2022**, *286*, 131648. [[CrossRef](#)]
100. Okazaki, Y.; Fujinaga, S.; Tanaka, A.; Kohzu, A.; Oyagi, H.; Nakano, S.I. Ubiquity and quantitative significance of bacterioplankton lineages inhabiting the oxygenated hypolimnion of deep freshwater lakes. *ISME J.* **2017**, *11*, 2279–2293. [[CrossRef](#)]
101. Hallbeck, L.; Pederson, K. The Family Gallionellaceae. In *The Prokaryotes*; Rosenberg, E., DeLong, E.F., Lory, S.S., Thompson, F., Eds.; Springer: Berlin/Heidelberg, Germany, 2014; pp. 853–858.
102. Dae-Kyun, P.; Maeng, J.; Ahn, C.-Y.; Chung, A.-S.; Lee, J.-H.; Oh, H.M. Geosmin Concentration and Its Relation to Environmental Factors in Daechung Reservoir, Korea. *Korean J. Limnol.* **2001**, *34*, 319–326.
103. Stoermer, E.F.; Julius, M.L. Centric Diatoms. In *Freshwater algae of North America—Ecology and Classification*; Wehr, J.D., Sheath, R.G., Eds.; Elsevier: Amsterdam, The Netherlands, 2003; pp. 559–594.
104. Maldonado, M.; Ribes, M.; van Duyl, F.C. Nutrient Fluxes Through Sponges: Biology, Budgets, and Ecological Implications. In *Advances in Marine Biology*; Becerro, M.A., Uriz, M.J., Maldonado, M., Turon, X., Eds.; Academic Press: Cambridge, MA, USA, 2012; pp. 113–182.
105. Xiao, Z.; Zhang, S.; Yan, P.; Huo, J.; Aurangzeib, M. Microbial Community and Their Potential Functions after Natural Vegetation Restoration in Gullies of Farmland in Mollisols of Northeast China. *Land* **2022**, *11*, 2231. [[CrossRef](#)]
106. Farkas, M.; Kaszab, E.; Radó, J.; Háhn, J.; Tóth, G.; Harkai, P.; Ferincz, Á.; Lovász, Z.; Táncsics, A.; Vörös, L.; et al. Planktonic and Benthic Bacterial Communities of the Largest Central European Shallow Lake, Lake Balaton and Its Main Inflow Zala River. *Curr. Microbiol.* **2020**, *77*, 4016–4028. [[CrossRef](#)] [[PubMed](#)]
107. Kozak, A.; Celewicz-Gołdyn, S.; Kuczyńska-Kippen, N. Cyanobacteria in small water bodies: The effect of habitat and catchment area conditions. *Sci. Total Environ.* **2019**, *646*, 1578–1587. [[CrossRef](#)] [[PubMed](#)]
108. Flores, E.; Herrero, A. Nitrogen assimilation and nitrogen control in cyanobacteria. *Biochem. Soc. Trans.* **2005**, *33*, 164–168. [[CrossRef](#)]
109. Saadoun, I.M.K.; Schrader, K.K.; Blevins, W.T. Environmental and nutritional factors affecting geosmin synthesis by *Anabaena* sp. *Water Res.* **2001**, *35*, 1209–1218. [[CrossRef](#)]
110. Collos, Y.; Berges, J. Nitrogen metabolism in phytoplankton. In *Marine Ecology*; Duarte, C.M., Lot Helgueras, A., Eds.; Encyclopaedia of Life Support Systems (EOLSS): Oxford, UK, 2003; pp. 262–280.
111. Clercin, N.A.; Koltsidou, I.; Picard, C.J.; Druschel, G.K. Prevalence of Actinobacteria in the production of 2-methylisoborneol and geosmin, over Cyanobacteria in a temperate eutrophic reservoir. *Chem. Eng. J. Adv.* **2022**, *9*, 100226. [[CrossRef](#)]
112. Hojun, L.; Depuydt, S.; Choi, S.; Kim, G.; Pandey, L.K.; Hader, D.P.; Han, T.; Park, J. Potential use of nuisance cyanobacteria as a source of anticancer agents. In *Natural Bioactive Compounds*; Sinha, R.P., Hader, D.P., Eds.; Academic Press: Cambridge, MA, USA, 2021; pp. 203–231.
113. Śliwińska-Wilczewska, S.; Maculewicz, J.; Felpeto, A.B.; Latała, A. Allelopathic and bloom-forming picocyanobacteria in a changing world. *Toxins* **2018**, *10*, 48. [[CrossRef](#)]
114. Khanh Tran, H.N.; Kim, J.A.; Youn, U.J.; Kim, S.; Woo, M.H.; Min, B.S. Investigation of chemical compounds from *Chlamydomonas* sp. KSF108 (Chlamydomonadaceae). *Biochem. Syst. Ecol.* **2019**, *83*, 4–6. [[CrossRef](#)]
115. Cattaneo, C.R.; Rodríguez, Y.; Rene, E.R.; García-Depraect, O.; Muñoz, R. Biogas bioconversion into poly(3-hydroxybutyrate) by a mixed microbial culture in a novel Taylor flow bioreactor. *Waste Manag.* **2022**, *150*, 364–372. [[CrossRef](#)]
116. Khairunisa, B.H.; Loganathan, U.; Ogejo, J.A.; Mukhopadhyay, B. Nitrogen Transformation Processes in Manure Microbiomes of Earthen Pit and Concrete Storages on Commercial Dairy Farms. *Res. Sq.* **2022**, *PREPRINT*, 1–24. [[CrossRef](#)]
117. Veraart, A.J.; Romaní, A.M.; Tornés, E.; Sabater, S. Algal response to nutrient enrichment in forested oligotrophic stream. *J. Phycol.* **2008**, *44*, 564–572. [[CrossRef](#)]
118. Thacker, M.; Karthick, B. Response of Diatoms to the Changing Water Quality in the Myristica Swamps of the Western Ghats, India. *Diversity* **2022**, *14*, 202. [[CrossRef](#)]

119. Tamura, T. The Family Sporichthyaceae. In *The Prokaryotes*, 4th ed.; Rosenberg, E., DeLong, E.F., Stackebrandt, E., Thompson, F., Eds.; Springer: Berlin/Heidelberg, Germany, 2014; pp. 883–888.
120. Deemer, B.R.; Harrison, J.A. Summer Redox Dynamics in a Eutrophic Reservoir and Sensitivity to a Summer 's End Drawdown Event. *Ecosystems* **2019**, *22*, 1618–1632. [[CrossRef](#)]
121. Lee, J.E.; Youn, S.J.; Byeon, M.; Yu, S.J. Occurrence of cyanobacteria, actinomycetes, and geosmin in drinking water reservoir in Korea: A case study from an algal bloom in 2012. *Water Sci. Technol. Water Supply* **2020**, *20*, 1862–1870. [[CrossRef](#)]
122. Luo, F.; Chen, H.; Wu, X.; Liu, L.; Chen, Y.; Wang, Z. Insights into the Seasonal Olfactory Mechanism of Geosmin in Raw Water of Huangpu River. *Toxics* **2022**, *10*, 485. [[CrossRef](#)]
123. Heudre, D.; Wetzel, C.E.; Moreau, L.; Van de Vijver, B.; Ector, L. On the identity of the rare fragilaria subconstricta (fragilariaceae), with fragilaria species forming ribbon-like colonies shortly reconsidered. *Plant Ecol. Evol.* **2019**, *152*, 327–339. [[CrossRef](#)]
124. Kulichevskaya, I.S.; Ivanova, A.O.; Belova, S.E.; Baulina, O.I.; Bodelier, P.L.E.; Rijpstra, W.I.C.; Sinninghe Damsté, J.S.; Zavarzin, G.A.; Dedysch, S.N. *Schlesneria paludicola* gen. nov., sp. nov., the first acidophilic member of the order Planctomycetales, from Sphagnum-dominated boreal wetlands. *Int. J. Syst. Evol. Microbiol.* **2007**, *57*, 2680–2687. [[CrossRef](#)]
125. Molot, L.A.; Watson, S.B.; Creed, I.F.; Trick, C.G.; McCabe, S.K.; Verschoor, M.J.; Sorichetti, R.J.; Powe, C.; Venkiteswaran, J.J.; Schiff, S.L. A novel model for cyanobacteria bloom formation: The critical role of anoxia and ferrous iron. *Freshw. Biol.* **2014**, *59*, 1323–1340. [[CrossRef](#)]

Disclaimer/Publisher's Note: The statements, opinions and data contained in all publications are solely those of the individual author(s) and contributor(s) and not of MDPI and/or the editor(s). MDPI and/or the editor(s) disclaim responsibility for any injury to people or property resulting from any ideas, methods, instructions or products referred to in the content.